Supplement of

Concentration and source changes of HONO during the COVID-19 lockdown in Beijing

Yusheng Zhang[1], Feixue Zheng[1], Zemin Feng[1,2], Chaofan Lian[3,4], Weigang Wang[3,4*], Xiaolong Fan[1,5,6], Wei Ma[1], Zhuohui Lin[1], Chang Li[1], Gen Zhang[7], Chao Yan[8,9], Ying Zhang[1,9], Veli-Matti Kerminen[1,8], Federico Bianch[1,8], Tuukka Petäjä[1,8], Juha Kangasluoma[1,8], and Markku Kulmala[1,8], Yongchun Liu[1*]

**Correspondence*: Yongchun Liu (liuyc@buct.edu.cn) and Weigang Wang (wangwg@iccas.ac.cn)

Table S1. Instruments used in the measurement.

Parameter	Instrument	Time resolution	Detection limit	Accuracy
HONO	LOPAP	60 s	0.01 ppb	10%
NO	Thermo Scientific 42i	60 s	0.05 ppb	5%
NO_2	Thermo Scientific 42i	60 s	0.05 ppb	5%
SO_2	Thermo Scientific 43i	60 s	0.12 ppb	5%
CO	Thermo Scientific 48i	60 s	40 ppb	5%
O_3	Thermo Scientific 49i	60 s	0.5 ppb	5%
$PM_{2.5}$	TEOM	300 s	0.05 μg m^{-3}	10%
Temperature	AWS310	60 s	-	1%
Relative humidity	AWS310	60 s	-	1%
Wind speed	AWS310	60 s	0.01 m s^{-1}	1%
Wind direction	AWS310	60 s	-	1%
UVB	AWS310	60 s	0.001 W m^{-2}	1%
J_{NO2}	2-pi-J_{NO2} radiometer	60 s	1.0×10^{-5} s^{-1}	1%
Boundary layer height	Ceilometer (CL51)	60 s	50 m	10%
Nitrate	ToF-ACSM	600 s	0.021 μg m^{-3}	5%
Sulfate	ToF-ACSM	600 s	0.018 μg m^{-3}	5%
Chloride	ToF-ACSM	600 s	0.011 μg m^{-3}	5%
Ammonium	ToF-ACSM	600 s	0.182 μg m^{-3}	5%
Organic	ToF-ACSM	600 s	0.198 μg m^{-3}	5%

Table S2. Sensitivity analysis with different parameters for the HONO budget

Method	Emission factor	OH	γ_{NO2} (ground)	γ_{NO2} (aerosol)	J_{NO3^-}	As	δ	$F_{HONO,soil}$	V_d	$K_{dilution}$	Sensitivity
M0	0.0109	CaV1[a]	2×10^{-6}	2×10^{-6}	8.24×10^{-5}	CaV2[b]	3.85	CaV3[c]	0.001	0.23	-
M1	0.008	CaV1	2×10^{-6}	2×10^{-6}	8.24×10^{-5}	CaV2	3.85	CaV3	0.001	0.23	-8%
M2	0.0186	CaV1	2×10^{-6}	2×10^{-6}	8.24×10^{-5}	CaV2	3.85	CaV3	0.001	0.23	20%
M3	0.0109	CaV1×0.1	2×10^{-6}	2×10^{-6}	8.24×10^{-5}	CaV2	3.85	CaV3	0.001	0.23	-24%
M4	0.0109	CaV1×2	2×10^{-6}	2×10^{-6}	8.24×10^{-5}	CaV2	3.85	CaV3	0.001	0.23	26%
M5	0.0109	CaV1	1×10^{-5}	2×10^{-6}	8.24×10^{-5}	CaV2	3.85	CaV3	0.001	0.23	40%
M6	0.0109	CaV1	2×10^{-7}	2×10^{-6}	8.24×10^{-5}	CaV2	3.85	CaV3	0.001	0.23	-9%
M7	0.0109	CaV1	2×10^{-6}	1×10^{-5}	8.24×10^{-5}	CaV2	3.85	CaV3	0.001	0.23	4%
M8	0.0109	CaV1	2×10^{-6}	2×10^{-7}	8.24×10^{-5}	CaV2	3.85	CaV3	0.001	0.23	-1%
M9	0.0109	CaV1	2×10^{-6}	2×10^{-6}	6.0×10^{-6}	CaV2	3.85	CaV3	0.001	0.23	-25%
M10	0.0109	CaV1	2×10^{-6}	2×10^{-6}	3.7×10^{-4}	CaV2	3.85	CaV3	0.001	0.23	95%
M11	0.0109	CaV1	2×10^{-6}	2×10^{-6}	8.24×10^{-5}	CaV2×0.1	3.85	CaV3	0.001	0.23	-1%

M12	0.0109	CaV1	2×10^{-6}	2×10^{-6}	8.24×10^{-5}	CaV2×10	3.85	CaV3	0.001	0.23	9%
M13	0.0109	CaV1	2×10^{-6}	2×10^{-6}	8.24×10^{-5}	CaV2	1	CaV3	0.001	0.23	-7%
M14	0.0109	CaV1	2×10^{-6}	2×10^{-6}	8.24×10^{-5}	CaV2	2.2	CaV3	0.001	0.23	-4%
M15	0.0109	CaV1	2×10^{-6}	2×10^{-6}	8.24×10^{-5}	CaV2	3.85	CaV3×0.1	0.001	0.23	-1%
M16	0.0109	CaV1	2×10^{-6}	2×10^{-6}	8.24×10^{-5}	CaV2	3.85	CaV3×10	0.001	0.23	4%
M17	0.0109	CaV1	2×10^{-6}	2×10^{-6}	8.24×10^{-5}	CaV2	3.85	CaV3	0.00077	0.23	1%
M18	0.0109	CaV1	2×10^{-6}	2×10^{-6}	8.24×10^{-5}	CaV2	3.85	CaV3	0.025	0.23	-24%
M19	0.0109	CaV1	2×10^{-6}	2×10^{-6}	8.24×10^{-5}	CaV2	3.85	CaV3	0.001	0.1	12%
M20	0.0109	CaV1	2×10^{-6}	2×10^{-6}	8.24×10^{-5}	CaV2	3.85	CaV3	0.001	0.44	-19%

Here CaV1[a], CaV2[b] and CaV3[c] represented the Calculated values of OH (according to Eq. (8)), *As* is the surface area concentration of aerosol and $F_{HONO,soil}$ is soil emission flux (Oswald et al., 2013). The emission factor and δ are based on measurements in our previous work (Liu et al., 2020b). J_{NO3^-} (Liu et al., 2020a), V_d (Han et al., 2017) and $K_{dilution}$ (Dillon et al., 2002) are from references, respectively. The γ_{NO2} for aerosol and ground surface are calculated using Eq. (3-7). M0 represents the parameterized scheme input for the base case. M1-M20 are sensitivity analyses for different parameters in the HONO budget analysis, respectively.

Table S3. Periods and mean values (mean ± standard deviation, (minimum to maximum value)) of wind speed, $PM_{2.5}$, RH, T, HONO, trace gas, and NR-$PM_{2.5}$ in field observation.

Category	BCNY	COVID
Periods	January 1 - January 24	January 25 - March 6
Wind speed (m/s)	0.64±0.42 (0.04-3.65)	0.80±0.55 (0.02-3.86)
$PM_{2.5}$ (μg/m^3)	47.23±44.50 (3-265)	69.86±67.26 (2-268)
RH (%)	36.79±14.66 (12-94)	45.14±21.20 (12-95)
T (°C)	0.89±2.98 (-7.5–9.9)	3.42±3.97 (-6.8-12.6)
HONO (ppb)	0.97±0.74 (0.17-3.85)	0.53±0.45 (0.01-2.11)
NO (ppb)	18.42±29.24 (0.03-162.92)	2.44±5.40 (0.01-51.08)
NO_2 (ppb)	26.99±13.41 (2.68-54.51)	17.26±11.34 (0.57-64.44)
NO_X (ppb)	45.35±38.90 (2.27-207.46)	19.52±14.41 (0.33-89.09)
CO (ppb)	907.72±499.16 (294.93-3013.30)	954.87±624.04 (242.24-3751.68)
SO_2 (ppb)	2.09±1.36 (0.03-8.56)	1.47±1.95 (0.01-14.25)
O_3 (ppb)	12.16±10.79 (0.38-37.90)	21.29±11.78 (0.56-60.69)
NO_3^- (μg/m^3)	9.99±9.72 (0.09-57.62)	16.71±18.20 (0.08-89.28)
SO_4^{2-} (μg/m^3)	4.59±7.08 (0.43-56.91)	7.99±8.61 (0.35-37.39)
NH_4^+ (μg/m^3)	4.95±5.08 (0.23-31.90)	9.24±10.32 (0.17-51.36)
Cl^- (μg/m^3)	1.22±1.24 (0.01-6.72)	1.42±1.53 (0.01-8.37)
OA (μg/m^3)	14.71±10.75 (0.88-60.54)	18.19±16.52 (0.88-77.28)

Table S4. Summaries for HONO concentration of field observation.

Location	Date	HONO	NO_2	NO	$PM_{2.5}$
This study	2020.1.1-2020.1.24	0.97±0.74	26.9±13.41	18.4±29.24	47.2±44.5
	2020.1.25-2020.3.6	0.53±0.44	17.2±11.34	2.43±5.39	69.9±67.2
Shijia Zhuang (Liu et al., 2020a)	2019.12.15-2020.1.22	2.43±1.08	31.7	26.3±26.2	137.9±85.8
Beijing (Liu et al., 2020b)	2018.2.1-2018.6.30	1.26±1.06			
Guangzhou (Li et al., 2012)	2006.7.3-2006.7.31	0.95(night) 0.24(day)	16.5(night) 4.5(day)		
Beijing (Spataro et al., 2013)	2007.1.23-2007.2.14	1.04±0.73	38.76±10.02		
	2007.8.2-2007.8.31	1.45±0.58	31.7±7.82		70.12±29.62
Hyytiälä.Finland (Oswald et al., 2015)	2010.7.12-2010.8.12	0.037(night) 0.027(day)			
Beijing (Tong et al., 2015)	2014.10.28-2014.12.2	1.45	37.4	44.4	
Hong Kong (Xu et al., 2015)	2011.8(Summer)	0.65	19.8	8	
	2011.11(Autumn)	0.93	26.8	10.1	
	2012.2(Winter)	0.91	24.7	19.3	

	2012.5(Spring)	0.35	15.5	5.5	
Beijing (Tong et al., 2016)	2015.12.12-2015.12.22	1.34(haze) 0.51(clean)	28.4(haze) 7.1(clean)	70.73(haze) 17.0(clean)	144 (haze) 29 (clean)
Xi'an (Huang et al., 2017)	2015.7.24-2015.8.6	1.12±0.97	20.9±11.0		
Beijing (Wang et al., 2017)	2015.9.22-10.21(Autumn)	2.27±1.82	32.91±20.44	38.79(night)	99.28(night)
	2016.1.3-1.27(Winter)	1.05±0.89	19.96±16.28	65.65(night)	95.75(night)
	2016.4.1-5.14(Spring)	1.05±0.95	25.97±15.8	21.39(night)	56.6(night)
	2016.6.20-7.25(Summer)	1.38±0.9	19.21±11.25	3.08(night)	49.55(night)
Shanghai (Cui et al., 2018)	2016.5.12-2016.5.28	2.31	46.46		
Ji'nan (Li et al., 2018)	2015.9-2015.11(Autumn)	0.87±0.66	25.4±23.2	12.6	
	2015.12-2016.2(Winter)	2.15±1.35	41.1±34.6	37.4	
	2016.3-2016.5(Spring)	1.24±1.04	35.8±25.8	11.5	
	2016.6-2016.8(Summer)	1.2±1.01	22.5±19.0	6.6	
Nanjing (Liu et al., 2019)	2017.12-2018.2(Winter)	1.15(night); 0.92(day)	28.4(night);23(day)	17.1(night);14.6(day)	
	2018.3-5 (Spring)	0.76(night);0.59 (day)	17.4(night);12.9(day)	1.7(night);3.0(day)	
	2018.6-8 (Summer)	0.56(night);0.34(day)	12.5(night);7.7(day)	1.0(night);1.4(day)	

	2018.9-11 (Autumn)	0.81(night);0.51(day)	18.9(night);13.4(day)	6.2(night);4.3(day)
Beijing (Zhang et al., 2019)	2016.12	3.5±2.7	56±23	67±48
	2016.12(clean)	0.5 ± 0.2	19 ± 9	5 ± 5
	2016.12(haze)	3.4 ± 1.7	60 ± 13	75 ± 39
	2016.12(severe haze)	5.8 ± 3.0	76 ± 14	94 ± 40
Nanjing (Zheng et al., 2020)	2015.12.1-12.31	1.32±0.92	23.9±7.5	
Beijing (Liu et al., 2021)	2018.5.25-7.15(Summer)	1.27 ± 0.44	18.98 ± 4.47	
	2018.11.26-2019.1.15(winter)	1.13 ± 0.68	19.99 ± 9.38	
Xiamen (Hu et al., 2022)	2018.8 (Summer)	0.51(night);0.72(day)	15.7(night);11.0(day)	3.2(night);5.6(day)
	2018.10 (Autumn)	0.33(night);0.50(day)	14.3(night);11.4(day)	0.8(night);2.7(day)
	2018.12 (Winter)	0.52(night);0.61(day)	18.3(night);15.8(day)	4.8(night);12.2(day)
	2019.3 (Spring)	0.51(night);0.72(day)	17.7(night);18.5(day)	6.8(night);10.1(day)
Guangzhou (Yu et al., 2022)	2018.9-11	0.91(night);0.44(day)	36.9(night);23.3(day)	10.8(night);6.8(day)

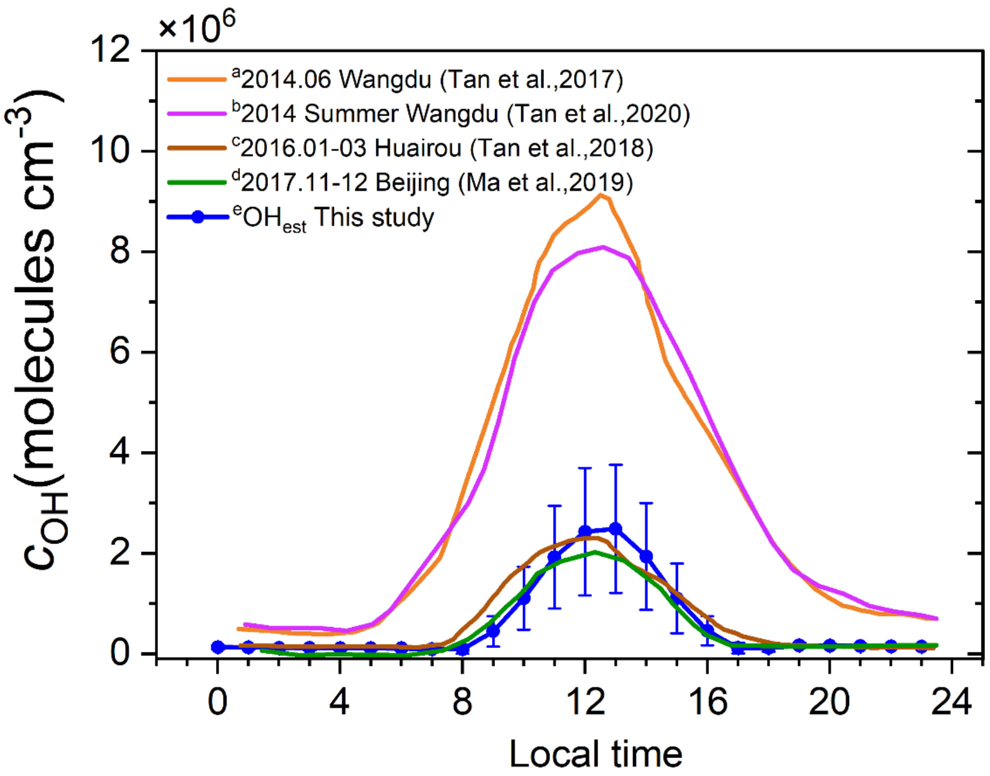

Figure S1. Diurnal variation of OH concentrations observed in different areas of the North China Plain (a-d) (Tan et al., 2017; Tan et al., 2018; Ma et al., 2019; Tan et al., 2020) and parameterized fitting in this study (e).

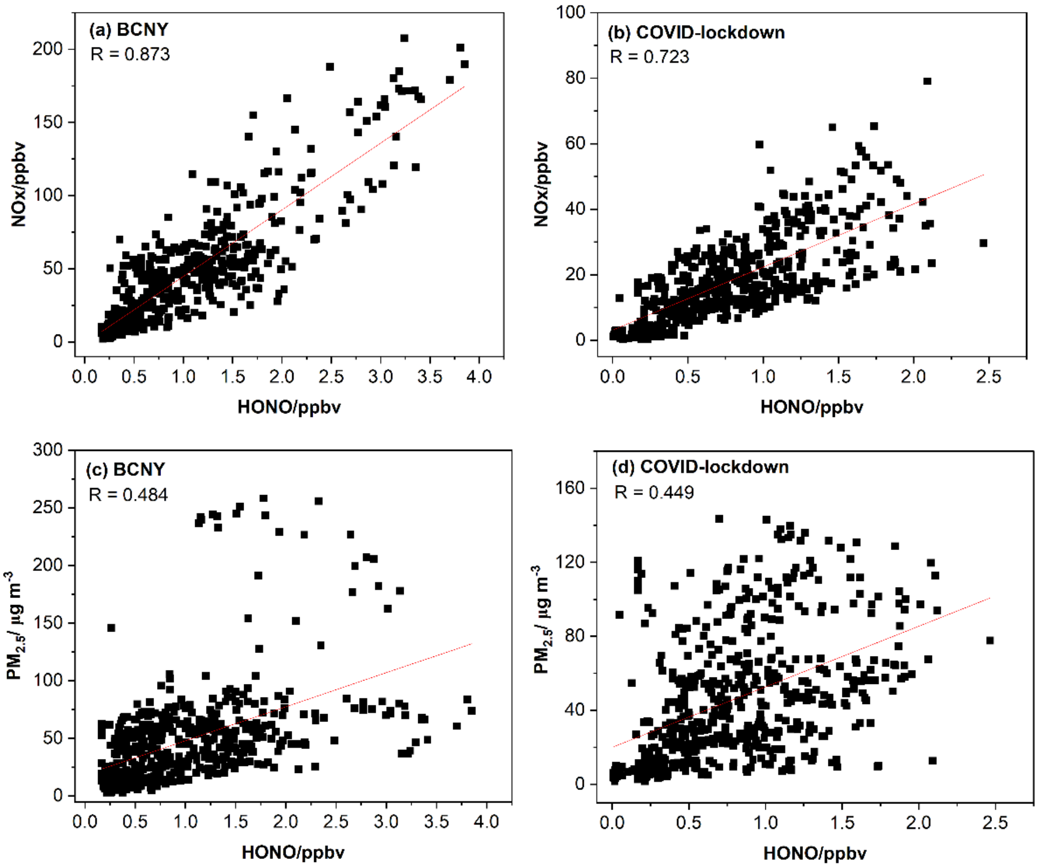

Figure S2. Correlation and scatterplot between HONO, NO_x (**a**: BCNY; **b**: COVID-lockdown) and $PM_{2.5}$ (**c**: BCNY; **d**: COVID-lockdown).

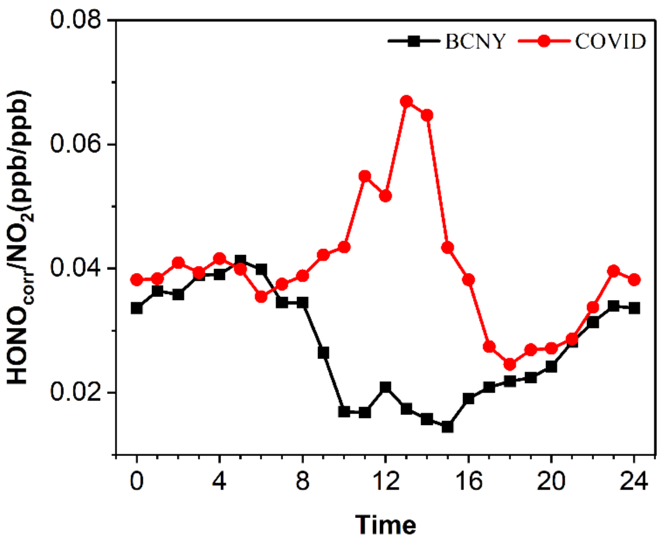

Figure S3. Diurnal variations of observed $HONO_{corr}/NO_2$ in BCNY (black line) and COVID (red line).

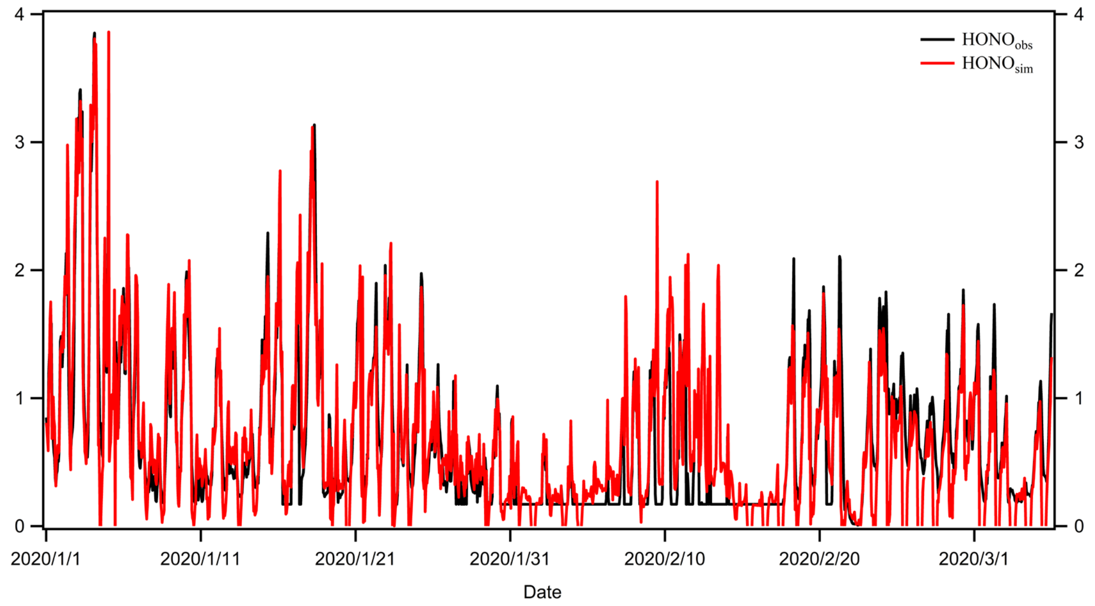

Figure S4. Comparison of simulated (HONO$_{sim}$, red line) and observed (HONO$_{obs}$, black line) hourly mean HONO concentration at the BUCT site over the period Jan. 1~Mar. 6, 2020.

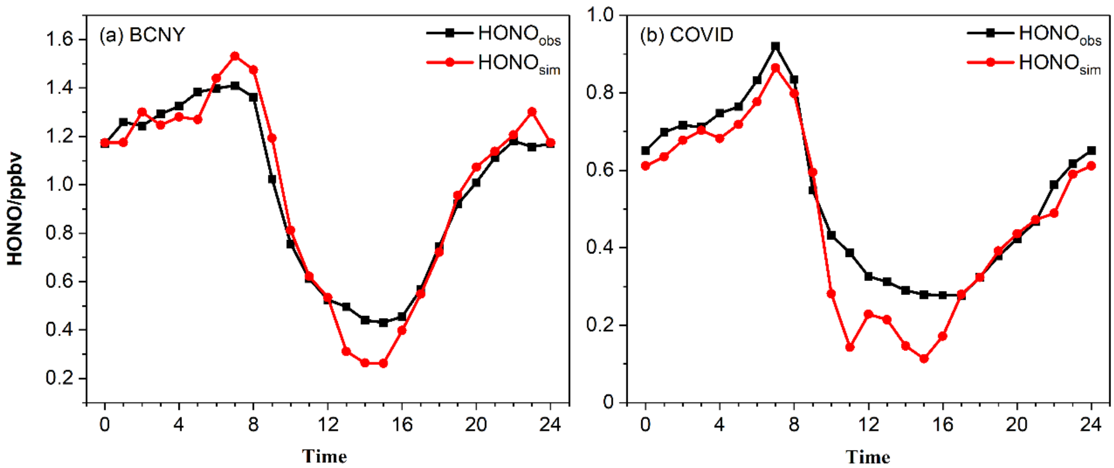

Figure S5. Observed and simulated HONO concentrations. Diurnal variations of observed HONO (HONO$_{obs}$, black line) and simulated HONO (HONO$_{sim}$, red line) in (**a**) BCNY and (**b**) COVID.

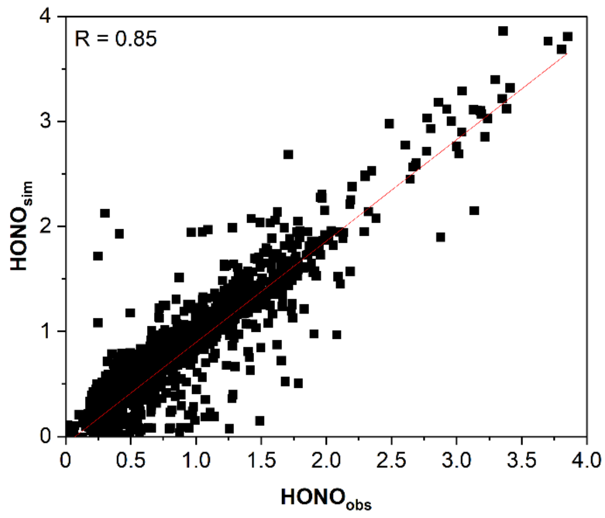

Figure S6. Correlation and Scatter plots between $HONO_{obs}$ and $HONO_{sim}$.

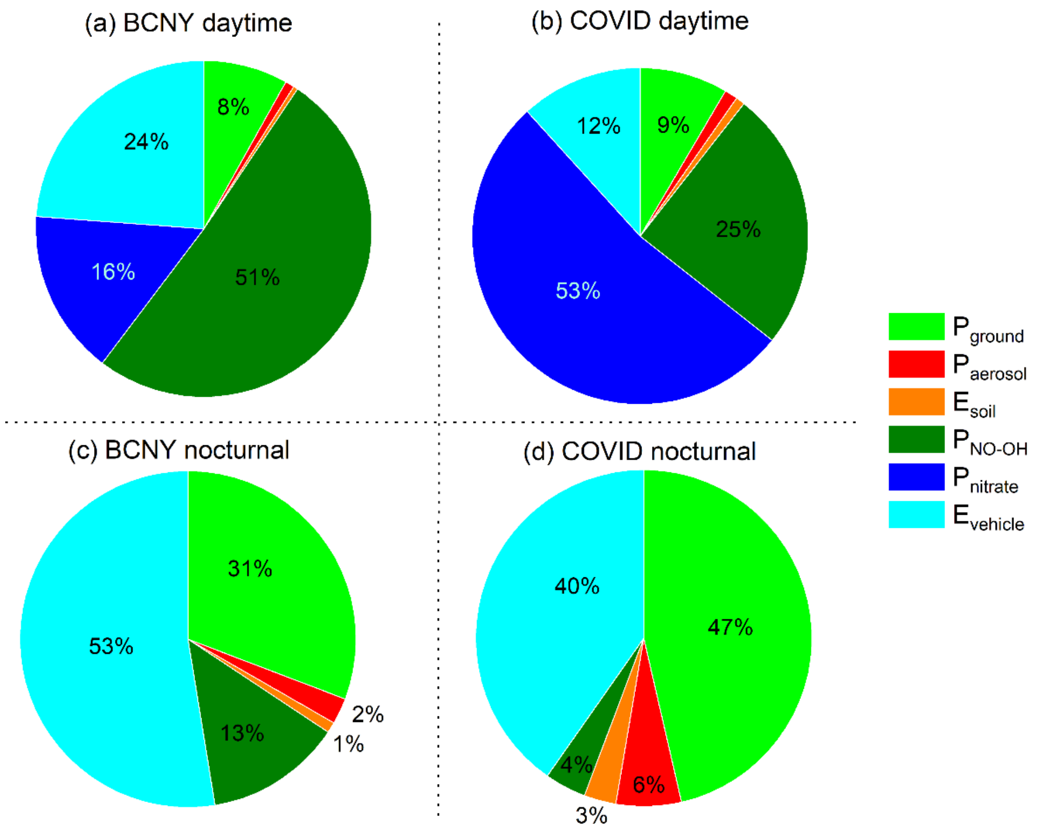

Figure S7. The percentage of daytime and nighttime contribution from different sources in (**a,c**) BCNY and (**b,d**) COVID.

Reference

Cui, L., Li, R., Zhang, Y., Meng, Y., Fu, H., and Chen, J.: An observational study of nitrous acid (HONO) in Shanghai, China: The aerosol impact on HONO formation during the haze episodes, Sci Total Environ, 630, 1057-1070, 10.1016/j.scitotenv.2018.02.063, 2018.

Dillon, M. B., Lamanna, M. S., Schade, G. W., Goldstein, A. H., and Cohen, R. C.: Chemical evolution of the Sacramento urban plume: Transport and oxidation, Journal of Geophysical Research: Atmospheres, 107, ACH 3-1-ACH 3-15, 10.1029/2001jd000969, 2002.

Han, X., Zhang, M., Skorokhod, A., and Kou, X.: Modeling dry deposition of reactive nitrogen in China with RAMS-CMAQ, Atmospheric Environment, 166, 47-61, 10.1016/j.atmosenv.2017.07.015, 2017.

Hu, B., Duan, J., Hong, Y., Xu, L., Li, M., Bian, Y., Qin, M., Fang, W., Xie, P., and Chen, J.: Exploration of the atmospheric chemistry of nitrous acid in a coastal city of southeastern China: results from measurements across four seasons, Atmospheric Chemistry and Physics, 22, 371-393, 10.5194/acp-22-371-2022, 2022.

Huang, R. J., Yang, L., Cao, J., Wang, Q., Tie, X., Ho, K. F., Shen, Z., Zhang, R., Li, G., Zhu, C., Zhang, N., Dai, W., Zhou, J., Liu, S., Chen, Y., Chen, J., and O'Dowd, C. D.: Concentration and sources of atmospheric nitrous acid (HONO) at an urban site in Western China, Sci Total Environ, 593-594, 165-172, 10.1016/j.scitotenv.2017.02.166, 2017.

Li, D., Xue, L., Wen, L., Wang, X., Chen, T., Mellouki, A., Chen, J., and Wang, W.: Characteristics and sources of nitrous acid in an urban atmosphere of northern China: Results from 1-yr continuous observations, Atmospheric Environment, 182, 296-306, 10.1016/j.atmosenv.2018.03.033, 2018.

Li, X., Brauers, T., Häseler, R., Bohn, B., Fuchs, H., Hofzumahaus, A., Holland, F., Lou, S., Lu, K. D., Rohrer, F., Hu, M., Zeng, L. M., Zhang, Y. H., Garland, R. M., Su, H., Nowak, A., Wiedensohler, A., Takegawa, N., Shao, M., and Wahner, A.: Exploring the atmospheric chemistry of nitrous acid (HONO) at a rural site in Southern China, Atmospheric Chemistry and Physics, 12, 1497-1513, 10.5194/acp-12-1497-2012, 2012.

Liu, J., Liu, Z., Ma, Z., Yang, S., Yao, D., Zhao, S., Hu, B., Tang, G., Sun, J., Cheng, M., Xu, Z., and Wang, Y.: Detailed budget analysis of HONO in Beijing, China: Implication on atmosphere oxidation capacity in polluted megacity, Atmospheric Environment, 244, 10.1016/j.atmosenv.2020.117957, 2021.

Liu, Y., Nie, W., Xu, Z., Wang, T., Wang, R., Li, Y., Wang, L., Chi, X., and Ding, A.: Semi-quantitative understanding of source contribution to nitrous acid (HONO) based on 1 year of continuous observation at the SORPES station in eastern China, Atmospheric Chemistry and Physics, 19, 13289-13308, 10.5194/acp-19-13289-2019, 2019.

Liu, Y., Ni, S., Jiang, T., Xing, S., Zhang, Y., Bao, X., Feng, Z., Fan, X., Zhang, L., and Feng, H.: Influence of Chinese New Year overlapping COVID-19 lockdown on HONO sources in Shijiazhuang, Sci Total Environ, 745, 141025, 10.1016/j.scitotenv.2020.141025, 2020a.

Liu, Y., Zhang, Y., Lian, C., Yan, C., Feng, Z., Zheng, F., Fan, X., Chen, Y., Wang, W., Chu, B., Wang, Y., Cai, J., Du, W., Daellenbach, K. R., Kangasluoma, J., Bianchi, F., Kujansuu, J., Petäjä, T., Wang, X., Hu, B., Wang, Y., Ge, M., He, H., and Kulmala, M.: The promotion effect of nitrous acid on aerosol formation in wintertime in Beijing: the possible contribution of traffic-related emissions, Atmospheric Chemistry and Physics, 20, 13023-13040, 10.5194/acp-20-13023-2020, 2020b.

Ma, X., Tan, Z., Lu, K., Yang, X., Liu, Y., Li, S., Li, X., Chen, S., Novelli, A., Cho, C., Zeng, L., Wahner, A., and Zhang, Y.: Winter photochemistry in Beijing: Observation and model simulation of OH and HO2 radicals at an urban site, Sci Total Environ, 685, 85-95, 10.1016/j.scitotenv.2019.05.329, 2019.

Oswald, R., Behrendt, T., Ermel, M., Wu, D., Su, H., Cheng, Y., Breuninger, C., Moravek, A., Mougin, E., Delon, C., Loubet, B., Pommerening-Roser, A., Sorgel, M., Poschl, U., Hoffmann, T., Andreae, M. O., Meixner, F. X., and Trebs, I.: HONO emissions from soil bacteria as a major source of atmospheric reactive nitrogen, Science, 341, 1233-1235, 10.1126/science.1242266, 2013.

Oswald, R., Ermel, M., Hens, K., Novelli, A., Ouwersloot, H. G., Paasonen, P., Petäjä, T., Sipilä, M., Keronen, P., Bäck, J., Königstedt, R., Hosaynali Beygi, Z., Fischer, H., Bohn, B., Kubistin, D., Harder, H., Martinez, M., Williams, J., Hoffmann, T., Trebs, I., and Sörgel, M.: A comparison of HONO budgets for two measurement heights at a field station within the boreal forest in Finland, Atmospheric Chemistry and Physics, 15, 799-813, 10.5194/acp-15-799-2015, 2015.

Spataro, F., Ianniello, A., Esposito, G., Allegrini, I., Zhu, T., and Hu, M.: Occurrence of atmospheric nitrous acid in the urban area of Beijing (China), Science of The Total Environment, 447, 210-224, 10.1016/j.scitotenv.2012.12.065, 2013.

Tan, Z., Hofzumahaus, A., Lu, K., Brown, S. S., Holland, F., Huey, L. G., Kiendler-Scharr, A., Li, X., Liu, X., Ma, N., Min, K. E., Rohrer, F., Shao, M., Wahner, A., Wang, Y., Wiedensohler, A., Wu, Y., Wu, Z., Zeng, L., Zhang, Y., and Fuchs, H.: No Evidence for a Significant Impact of Heterogeneous Chemistry on Radical Concentrations in the North China Plain in Summer 2014, Environ Sci Technol, 54, 5973-5979, 10.1021/acs.est.0c00525, 2020.

Tan, Z., Fuchs, H., Lu, K., Hofzumahaus, A., Bohn, B., Broch, S., Dong, H., Gomm, S., Häseler, R., He, L., Holland, F., Li, X., Liu, Y., Lu, S., Rohrer, F., Shao, M., Wang, B., Wang, M., Wu, Y., Zeng, L., Zhang, Y., Wahner, A., and Zhang, Y.: Radical chemistry at a rural site (Wangdu) in the North China Plain: observation and model calculations of OH, HO2 and RO2 radicals, Atmospheric Chemistry and Physics, 17, 663-690, 10.5194/acp-17-663-2017, 2017.

Tan, Z., Rohrer, F., Lu, K., Ma, X., Bohn, B., Broch, S., Dong, H., Fuchs, H., Gkatzelis, G. I., Hofzumahaus, A., Holland, F., Li, X., Liu, Y., Liu, Y., Novelli, A., Shao, M., Wang, H., Wu, Y., Zeng, L., Hu, M., Kiendler-Scharr, A., Wahner, A., and Zhang, Y.: Wintertime photochemistry in Beijing: observations of ROx radical concentrations in the North China Plain during the BEST-ONE campaign, Atmospheric Chemistry and Physics, 18, 12391-12411, 10.5194/acp-18-12391-2018, 2018.

Tong, S., Hou, S., Zhang, Y., Chu, B., Liu, Y., He, H., Zhao, P., and Ge, M.: Comparisons of measured nitrous acid (HONO) concentrations in a pollution period at urban and suburban Beijing, in autumn of 2014, Science China Chemistry, 58, 1393-1402, 10.1007/s11426-015-5454-2, 2015.

Tong, S., Hou, S., Zhang, Y., Chu, B., Liu, Y., He, H., Zhao, P., and Ge, M.: Exploring the nitrous acid (HONO) formation mechanism in winter Beijing: direct emissions and heterogeneous production in urban and suburban areas, Faraday Discuss, 189, 213-230, 10.1039/c5fd00163c, 2016.

Wang, J., Zhang, X., Guo, J., Wang, Z., and Zhang, M.: Observation of nitrous acid (HONO) in Beijing, China: Seasonal variation, nocturnal formation and daytime budget, Sci Total Environ, 587-588, 350-359, 10.1016/j.scitotenv.2017.02.159, 2017.

Xu, Z., Wang, T., Wu, J., Xue, L., Chan, J., Zha, Q., Zhou, S., Louie, P. K. K., and Luk, C. W. Y.: Nitrous acid (HONO) in a polluted subtropical atmosphere: Seasonal variability, direct vehicle emissions and heterogeneous production at ground surface, Atmospheric Environment, 106, 100-109, 10.1016/j.atmosenv.2015.01.061, 2015.

Yu, Y., Cheng, P., Li, H., Yang, W., Han, B., Song, W., Hu, W., Wang, X., Yuan, B., Shao, M., Huang, Z., Li, Z., Zheng, J., Wang, H., and Yu, X.: Budget of nitrous acid (HONO) at an urban site in the fall season of Guangzhou, China, Atmospheric Chemistry and Physics, 22, 8951-8971, 10.5194/acp-22-8951-2022, 2022.

Zhang, W., Tong, S., Ge, M., An, J., Shi, Z., Hou, S., Xia, K., Qu, Y., Zhang, H., Chu, B., Sun, Y., and He, H.: Variations and sources of nitrous acid (HONO) during a severe pollution episode in Beijing in winter 2016, Sci Total Environ, 648, 253-262, 10.1016/j.scitotenv.2018.08.133, 2019.

Zheng, J., Shi, X., Ma, Y., Ren, X., Jabbour, H., Diao, Y., Wang, W., Ge, Y., Zhang, Y., and Zhu, W.: Contribution of nitrous acid to the atmospheric oxidation capacity in an industrial zone in the Yangtze River Delta region of China, Atmospheric Chemistry and Physics, 20, 5457-5475, 10.5194/acp-20-5457-2020, 2020.